

Sinusoidal wavelength-scanning interferometer for measurement of thickness and surface profile of thin films

Hisashi Akiyama^a, Osami Sasaki^b, and Takamasa Suzuki^b

^aGraduate School of Science and Technology, Niigata University, Niigata-shi 950-2181, Japan

^bFaculty of Engineering, Niigata University, Niigata-shi 950-2181, Japan

ABSTRACT

We propose a sinusoidal wavelength scanning interferometer for measuring thickness and surfaces profiles with a thin film. An acousto-optic tunable filter (AOTF) is used to produce sinusoidally wavelength-scanned light from a superluminescent laser diode (SLD) with a wide spectral bandwidth of 46nm. The interference signal contains an amplitude Z_b of a time-varying phase and a constant phase α . Two measured values of OPD, which are denoted by L_z and L_α , are obtained from Z_b and α . By combining L_z and L_α , an OPD longer than a wavelength is measured with an error less than a few nanometers. When the object has two reflective surfaces, the detected interference signal contains two interference signals which are caused by the front and rear surfaces. In this case we must determine the values of Z_{b1} , Z_{b2} , α_1 , and α_2 , where suffixes of 1 and 2 are corresponding to the front and rear surfaces, respectively. We define an error function that is the difference between the detected signal and the theoretical signal, and reduce the value of the error function with the multidimensional nonlinear least-squares algorithm to search the values of Z_{b1} , Z_{b2} , α_1 , and α_2 . Experimental results show that the thickness and surfaces profiles of a silica glass plate of 20 μm -thickness are measured with error less than 1.5nm.

Keywords: Interferometer, surface profile, thickness, wavelength-scanning, sinusoidal phase-modulation.

1. INTRODUCTION

White light interferometry and wavelength-scanning interferometry are two basic methods for measuring thickness and surfaces profiles. In white light interferometry, the thickness of an object is measured by finding a position where the amplitude of the interference signal is maximum by scanning the optical path difference (OPD).¹⁾ In wavelength-scanning interferometry, the thickness of the object is measured by detecting a phase of the interference signal which varies with the scanning of the wavelength instead of the scanning of the OPD.²⁾ When the thickness of the object is very thin, in white light interferometry the peaks of the amplitude of the interference signal caused by the two reflecting surfaces, respectively, are overlapped so that it is difficult to distinguish the positions of the two peaks. Similarly in wavelength-scanning interferometry, the two peaks of the frequency spectrum of the interference signals caused by the two reflecting surfaces are overlapped. Therefore these conventional signal processing for finding the peaks are not suitable to measure the two reflecting surfaces of a very thin object. In Ref. 3, a linear wavelength-scanning interferometer using a white light and an acousto-optic tunable filter (AOTF) was used to obtain the scanning width of about 100nm. An error function was defined as the difference between the detected phase distribution and the theoretical one. By minimizing the error function, values related to the surfaces profiles and the thickness of the object were estimated for the thickness more than 0.1 μm . However a large scanning width of wavelength leads to measurement error due to the wavelength dispersion.

In this paper we propose a sinusoidal-wavelength scanning interferometer and a method of signal processing. The interference signal contains a phase changing sinusoidally and a constant phase α . The amplitude of the changing phase is called modulation amplitude Z_b which is proportional to the OPD and the wavelength scanning width. When the measurement error ϵ_{Lz} of Z_b is smaller than a half wavelength, by combining the two values of OPD obtained from the phase α and the modulation amplitude Z_b , the OPD longer than a wavelength can be measured with a few nanometers.⁴⁾ Using the light source with a large scanning width of wavelength is more easily to satisfy the condition that ϵ_{Lz} is smaller than a half wavelength. In experiments, we use a superluminescent laser diode (SLD) with a wide spectral bandwidth of 46nm and an AOTF to achieve a large wavelength-scanning width of 40nm. Combination of Z_b and α is used to

determine the positions of the two reflecting surfaces of an object. The error function is defined as the difference between the detected signal and the theoretical signal. Rough values of Z_b and α are obtained with double sinusoidal phase-modulating interferometry.⁵⁾ These values are used as the initial values for the process of signal estimation to obtain the real values of Z_b and α by minimizing the value of the error function. Experimental results of the thickness distribution and surfaces profiles of a silica glass plate of 20 μm -thickness are measured with an error less than 1.5nm.

2. PRINCIPLE

Figure 1 shows an interferometer for measuring thickness and profiles of a thin film. The output light of the SLD is collimated by lens L1 and incident on the AOTF. The wavelength of first-order reflection light from the AOTF is proportional to the frequency of the applied signal. Modulating the frequency sinusoidally, the wavelength of the light from the AOTF is scanned, as follows:

$$\lambda(t) = \lambda_0 + b \cos(\omega_b t), \quad (1)$$

where λ_0 is the central wavelength. The intensity of the light source is also changed, and it is denoted by $M(t)$. The light is divided into an object light and a reference light by a beam splitter (BS). The reference light is sinusoidally phase modulated with a vibrating mirror M1 whose movement is expressed as $a \cos(\omega_c t + \theta)$.

The object light is incident onto an object which has two surfaces A and B. Two reflected lights forms an image field with lens L2 and L3 on a two-dimensional CCD image sensor. OPDs between the two lights reflected by surface A and B and the reference light are denoted by L_1 and L_2 , respectively. The amplitudes of the two interference signals caused by surface A and B are denoted by a_1 and a_2 . Interference signal $S(t)$ detected with the CCD image sensor is given by

$$S(t) = M(t) + M(t) \sum_i a_i \cos [Z_i \cos(\omega_c t + \theta) + Z_{bi} \cos(\omega_b t) + \alpha_i] \quad (i=1,2) \quad (2)$$

where

$$\begin{aligned} Z_c &= 4\pi a / \lambda_0, \\ Z_{bi} &= 2\pi b L_i / \lambda_0^2, \\ \alpha_i &= 2\pi L_i / \lambda_0, \end{aligned} \quad (3)$$

and $i=1$ and 2 correspond to surface A and B, respectively. The intensity modulation $M(t)$ is obtained by detecting the reference light intensity. By dividing signal $S(t)$ by the known value of $M(t)$ and making Fourier transform of $S(t)/M(t)$, we obtain

$$\begin{aligned} A_c(t) &= A \sin \Phi(t) = \sum_i a_i \sin [Z_{bi} \cos(\omega_b t) + \alpha_i], \\ A_s(t) &= A \cos \Phi(t) = \sum_i a_i \cos [Z_{bi} \cos(\omega_b t) + \alpha_i], \end{aligned} \quad (i=1,2) \quad (4)$$

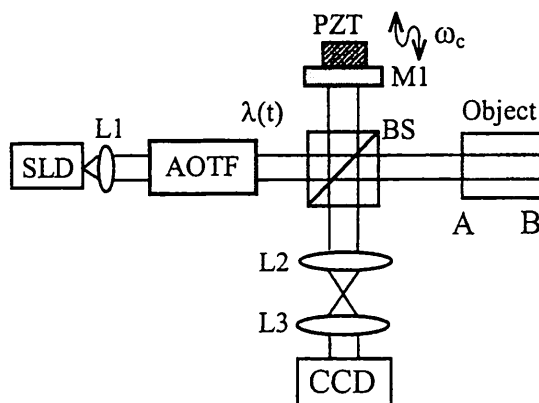


Fig. 1 Interferometer for measuring thickness and surface profiles of thin film.

in the same way described in Ref.6. The detected values of $A_s(t_m)$ and $A_c(t_m)$ are obtained from the detected interference signals, where $t_m=m\Delta t$. Since the refractive index of the object is known beforehand, the constant ratio K of a_1 to a_2 can be calculated. Using the detected values of $A_s(t_m)$, $A_c(t_m)$, and a known value of K , we define an error function

$$H=\sum_m \left\{ \left[\hat{A}_s(t_m)-A_s(t_m) \right]^2 + \left[\hat{A}_c(t_m)-A_c(t_m) \right]^2 \right\}, \quad (5)$$

where $\hat{A}_s(t_m)$ and $\hat{A}_c(t_m)$ are the estimated signals which contain unknowns of a_1 , Z_{bi} , and α_i ($i=1, 2$). The values of unknowns of a_1 , Z_{bi} , and α_i are searched to minimize H by multidimensional nonlinear least-squares algorithm.

We obtain values of L_i from the values of Z_{bi} that is denoted by L_{zi} , and also obtain other values of L_i from the values of α_i that is denoted by $L_{\alpha i}$. Since the measurement range of $\alpha_i=2\pi L_{\alpha i}/\lambda_0$ is limited $-\pi$ to π , a value of $L_{\alpha i}$ is limited to the range from $-\lambda_0/2$ to $\lambda_0/2$. On the other hand, a value of $Z_{bi}=2\pi b L_{zi}/\lambda_0^2$ provides a rough value L_{zi} of L_i . To combine L_{zi} and $L_{\alpha i}$, the following equation is used:

$$m_{ci}=(L_{zi}-L_{\alpha i})/\lambda_0. \quad (6)$$

If the measurement error $\epsilon_{L_{zi}}$ in L_{zi} is smaller than $\lambda_0/2$, a fringe order m_i is obtained by rounding off m_{ci} . When an OPD L_i is longer than a wave length, it is given by

$$L_i=m_i\lambda_0+L_{\alpha i}, \quad (7)$$

Since the measurement accuracy of $L_{\alpha i}$ is a few nanometers, an OPD over several ten micrometers can be measured with a high accuracy. The suffixes of $i=1$ and 2 in the L_{zi} , $L_{\alpha i}$, m_{ci} , and m_i correspond to surface A and B, respectively.

The front surface profile r_1 and rear surface profile r_2 are obtained from the estimated values of α_i as follows:

$$r_1=(\lambda_0/4\pi)\alpha_1, \quad r_2=(\lambda_0/4\pi n_R)[(n_R-1)\alpha_1+\alpha_2], \quad (8)$$

where n_R is the refractive index of the object and is constant in the object. From the estimated values of Z_{bi} , and α_i , the values of L_{zi} , and $L_{\alpha i}$ are obtained with Eqs.(3). Using Eq.(6) the values of m_1 and m_2 are obtained for the front and rear surfaces, respectively. Putting $m=m_2-m_1$, the thickness d is given by

$$d=(m\lambda_0/2n_R)+(r_2-r_1) \quad (9)$$

Thus we can measure thickness and two surface profiles.

3. EXPERIMENTAL SETUP

We tried to measure the front and rear surface profiles of a silica glass plate with a thickness of 20 μm . The refractive index n_R of the silica glass was 1.46. The ratio K of a_1 to a_2 was 0.96. The central wavelength λ_0 of the light source was 837.1 nm, and its spectral bandwidth was 46 nm. The wavelength-scanning width $2b$ was 40.0 nm. The spectral width of the first-order reflection light from the AOTF was about 3 nm. The wave scanning frequency of $\omega_b/2\pi$ and the phase modulating frequency of $\omega_c/2\pi$ were 15.8 and 506 Hz, respectively. When the absolute value of Z_{bi} increases, the spectra around the carrier frequencies of ω_c and $2\omega_c$ have a wider band. Maximum detectable absolute value of Z_{bi} depends on the ratio of the ω_c/ω_b . In contrast, when the absolute value of Z_{bi} decrease, the magnitude of the spectra around ω_c and $2\omega_c$ becomes so small that they can not be distinguished from noise. Therefore the absolute value of Z_{bi} must be between 2rad and 12rad at $\omega_c=32\omega_b$. When $b=20\text{nm}$ and $L_{z2}-L_{z1}=60\mu\text{m}$, the difference between the values of Z_{b1} and Z_{b2} was almost equal to 11rad. If the reference plane decided by the position of the reference mirror was outside of the object, it was difficult to satisfy the condition of $2\leq Z_{bi}\leq 12$. Therefore the reference plane was located inside of the object, and it was assumed that the OPD L_1 and L_2 were positive and negative values, respectively. Lens L2 and L3 formed an image of the object on the CCD image sensor with magnification of 2/3. A two-dimensional CCD image sensor was used to detect the interference signals. Number of the measuring point was 60×20 in a region of $1.8\text{mm} \times 0.6\text{mm}$ on the object surfaces along the x and y axes, respectively. Intervals of the measuring points were $\Delta x=30\mu\text{m}$ and $\Delta y=30\mu\text{m}$. Positions of the pixels of the CCD image sensor are denoted by l_x and l_y , respectively.

4. SIGNAL ESTIMATION

After the detected interference signals were processed to obtain $A_s(t)$ and $A_c(t)$ given by Eqs.(4), the error function given by Eq.(5) was minimized in the process of signal estimation. While searching for the real values of the unknowns, existences of a lot of local minima were found. The conditions of the initial values were examined by computer simulations. The initial values move to the real values almost certainly when differences between the initial values and the real values are within the following values: about 2rad for Z_{b1} and Z_{b2} , about 1.5rad for α_1 and α_2 , and about 50% accuracy for a_1 . However if one of these condition for the differences was not satisfied, the initial values do not always reach the global minimum. It was made clear from the simulations that good initial values were required to reach the global minimum in a short time.

First we tried to find better initial value of a_1 . We adjusted the position of the object by means of a micrometer so that OPD $L_1 \cdot \theta$. In this case Eqs.(4) is reduced to

$$\begin{aligned} A_s(t) &= Ka_1 \sin[Z_{b2} \cos(\omega_b t) + \alpha_2] + C_1, \\ A_c(t) &= Ka_1 \cos[Z_{b2} \cos(\omega_b t) + \alpha_2] + C_2, \end{aligned} \quad (10)$$

where $C_1 = a_1 \sin \alpha_1$ and $C_2 = a_1 \cos \alpha_1$ are constant. Since the terms of C_1 and C_2 is constant with time, they could be eliminated from Eqs.(10). Then the amplitude of the signals of $A_s(t)$ and $A_c(t)$ were changed from Ka_1 to $-Ka_1$. Since K was known value, a value of a_1 was obtained as the initial value. In this method the value of a_1 was obtained with about 20% accuracy, because the intensity modulation $M(t)$ and the constant terms of C_1 and C_2 could not be eliminated completely. Next we tried to find the initial value of Z_{b1} and Z_{b2} . Equations.(10) without terms of C_1 and C_2 are the same as those in the double sinusoidal phase-modulating interferometry.⁵⁾ Using the signal processing of double sinusoidal phase modulating interferometry for Eqs.(10), the value of Z_{b2} can be calculated with an error less than 1rad. In this method, the calculated value of Z_{b2} was -11rad at $Z_{b1} \cdot \theta$. Since the absolute values of Z_{bi} must be between 1rad and 12rad, the value of L_1 was changed from 0 to $16 \mu\text{m}$ by adjusting the position of the object. Then the initial values of Z_{b1} and Z_{b2} were 3rad and -8rad in the relation of $Z_{bi}(\text{rad}) = 0.179 \times L_i(\mu\text{m})$, respectively. On the other hand the initial values of α_1 and α_2 can not be obtained from the detected signals. Therefore the initial value of α_1 was given at intervals of 1.0rad in the range from $-\pi$ to π rad for the initial value of $\alpha_2 = 0$. When a global minimum could not be obtained, the initial value of α_2 was changed by 1.0 rad and the search was repeated again. Considering all combinations of α_1 and α_2 , the search became successful at most after 36 repetitions. The values estimated first at one measuring point were used as the initial values of the adjacent measuring points, because the difference in real values of α_1 and α_2 between the adjacent measuring points was within $\pi/2$ to detect the interference signal with a good amplitude.

5. MEASUREMENT RESULT

The values of L_{zi} , $L_{\alpha i}$, and m_{ci} were calculated from the estimated values of Z_{b1} , Z_{b2} , α_1 , and α_2 with Eqs.(3) and (4). Figure 2 shows the OPD L_{zi} calculated from Z_{bi} with Eqs.(3). Figure 3 also shows the OPD $L_{\alpha i}$ calculated from α_i with Eqs.(3). By combining L_{zi} and $L_{\alpha i}$ with Eq.(6), the fringe order m_1 and m_2 were calculated as shown in Fig.4. Table I shows the measured value of L_{zi} , $L_{\alpha i}$ and m_{ci} along I_x at $I_y = 10$. Figure 4 shows that fringe order m_1 of the front surface was 18 on all of the measuring points and fringe order m_2 of the rear surface was -49 on almost of the measuring points. Considering that the estimated phase of the rear surface changed smoothly as shown in Fig.3, it was assumed that fringe order m_2 of -50 was due to the measurement error caused by a noise. Therefore, we decided that front surface fringe order was 18 and rear surface fringe order was -49. Figure 5 show the front and rear surfaces of the object calculated from the estimated values of α_1 and α_2 with Eqs.(8). Figure 6 shows the thickness distribution calculated from r_1 , r_2 and $m=67$ with Eq.(9). The measurement accuracy of the thickness is equal to the measurement accuracy of surfaces profiles. We repeated the

Table I. Measured values along one line of I_x at $I_y=10$.

I_x	$L_{z1}(\mu\text{m})$	$L_{z2}(\mu\text{m})$	$L_{\alpha 1}(\mu\text{m})$	$L_{\alpha 2}(\mu\text{m})$	m_{c1}	m_{c2}
10	15.18	-40.74	0.145	0.335	18.0	-49.0
20	15.49	-40.67	0.285	0.497	18.2	-49.1
30	15.49	-40.74	0.355	0.588	18.1	-49.3
40	15.34	-40.70	0.336	0.600	17.9	-49.3
50	15.16	-40.56	0.235	0.535	17.8	-49.0
60	14.89	-40.83	0.061	0.388	17.7	-49.2

measurement of surface profiles five times to examine measurement repeatability. From these measurements the repeatability was about 1.5nm for front and rear surface.

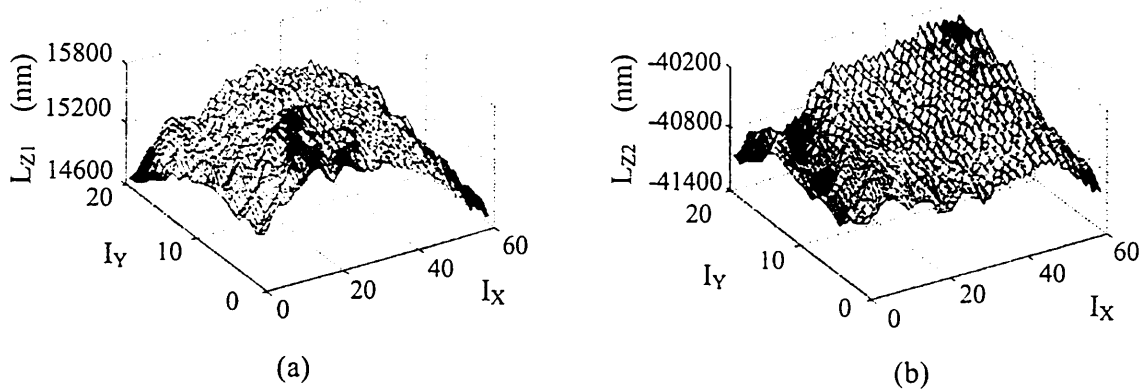


Fig. 2 Measured OPD L_{zi} calculated from Z_{bi} of the (a) front surface and (b) rear surface.

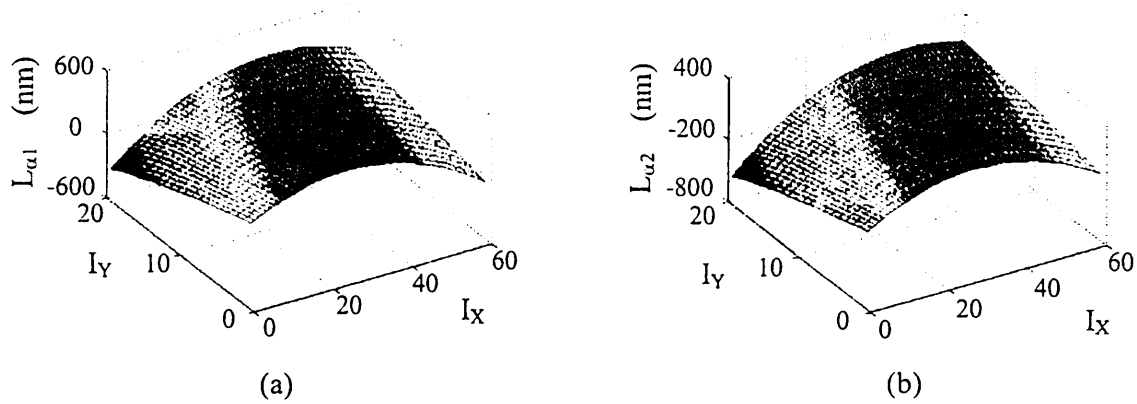


Fig. 3 Measured OPD $L_{\alpha i}$ calculated from α_i of the (a) front surface and (b) rear surface.

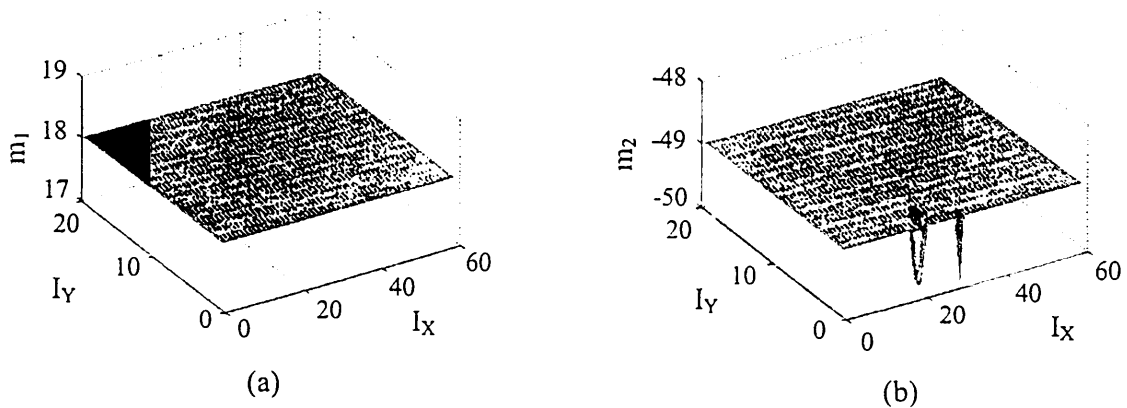


Fig. 4 Distribution of the fringe order (a) m_1 and (b) m_2 .

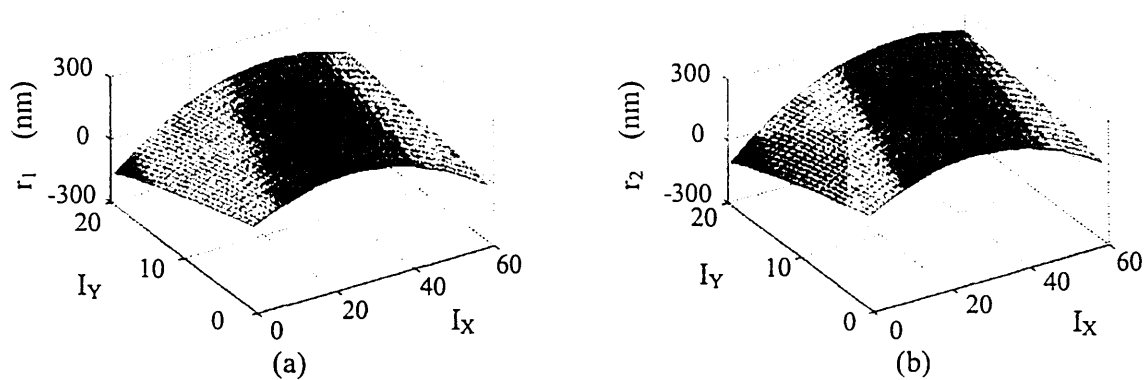


Fig. 5 Measured profiles of the (a) front surface and (b) rear surface.

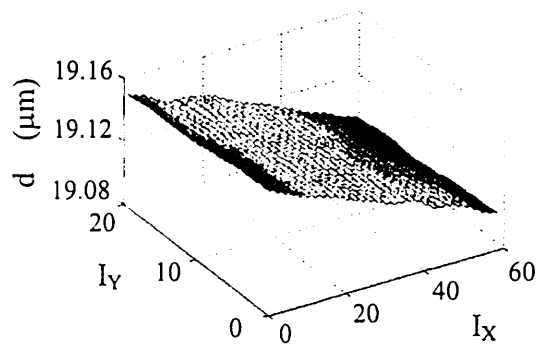


Fig. 6 Measured thickness between the two surfaces.

6. CONCLUSIONS

We have proposed a sinusoidal wavelength-scanning interferometer for measuring thickness and surface profiles of a thin film in which we used the SLD and the AOTF. The interference signal contains amplitude of the phase modulation Z_b and conventional phase α related to the thickness and surfaces profiles. We estimated values of Z_b and α by reducing the difference between the detected signal and the estimated signal. By combining the values of Z_b and α , the front and rear surfaces of a silica glass plate of $20\mu\text{m}$ -thickness could be measured with an error less than 1.5nm .

REFERENCES

1. H. Maruyama, S. Inoue, T. Mitsuyama, M. Ohmi and M. Haruna: Low-coherence interferometer system for the simultaneous measurement of refractive index and thickness, *Appl. Opt.* 41, (2002), 1315.
2. T. Funaba, N. Tanno and H. Ito: Multimode-laser reflectometer with a multichannel wavelength detector and its application, *Appl. Opt.* 36, (1997), 8919.
3. D. Kim, S. Kim, H. J. Kong and Y. Lee: Measurement of the thickness profile of a transparent thin film deposited upon a pattern structure with an acousto-optic tunable filter, *Opt. Lett.* 27, (2002), 1893.
4. O. Sasaki, K. Tsuji, S. Sato, T. Kuwahara and T. Suzuki: Sinusoidal wavelength-scanning interferometers, in *Laser Interferometry IX: techniques and Analysis*, M. Kujawinska, G. M. Brown, and M. Takeda, eds., Proc. SPIE 3478, (1998), 37.
5. O. Sasaki, T. Yoshida and T. Suzuki: Double sinusoidal phase-modulating laser diode interferometer for distance measurement, *Appl. Opt.* 30, (1991), 3617.
6. H. Akiyama, O. Sasaki and T. Suzuki: Thickness and surface profile measurement by a sinusoidal wavelength-scanning interferometer, *ICO'04*, (2004), 419